© 2018. Published by The Company of Biologists Ltd | Journal of Experimental Biology (2018) 221, jeb185710. doi:10.1242/jeb.185710

METHODS AND TECHNIQUES

Silencing cuticular pigmentation genes enables RNA FISH in intact insect appendages

Stefan Pentzold[1,*], Veit Grabe[2], Andrei Ogonkov[1], Lydia Schmidt[1], Wilhelm Boland[1] and Antje Burse[1]

ABSTRACT

Optical imaging of gene expression by fluorescence *in situ* hybridisation (FISH) in insects is often impeded by their pigmented cuticle. As most chemical bleaching agents are incompatible with FISH, we developed an RNA interference (RNAi)-based method for clearing cuticular pigmentation which enables the use of whole-mount body appendages for RNA FISH (termed RNA-i-FISH). Silencing *laccase2* or *tyrosine hydroxylase* in two leaf beetles species (*Chrysomela populi* and *Phaedon cochleariae*) cleared their pigmented cuticle and decreased light absorbance. Subsequently, intact appendages (palps, antennae, legs) from RNAi-cleared individuals were used to image the expression and spatial distribution of antisense mRNA of two chemosensory genes encoding gustatory receptor and odorant-binding protein. Imaging did not work for RNAi controls because the pigmentation was retained, or for FISH controls (sense mRNA). Several bleaching agents were incompatible with FISH, because of degradation of RNA, lack of clearing efficacy or long incubation times. Overall, silencing pigmentation genes is a significant improvement over bleaching agents, enabling FISH in intact insect appendages.

KEY WORDS: Beetle cuticle, RNA interference, Laccase2, Tyrosine hydroxylase, Whole-mount, Fluorescence *in situ* hybridisation, Gustatory receptor, Odorant-binding protein

INTRODUCTION

Optical imaging in combination with *in situ* fluorescence labelling is a powerful method to elucidate spatiotemporal patterns of gene expression and to identify cellular circuits in biological systems (Lampasona and Czaplinski, 2016). For optimal image sharpness and resolution in fluorescence microscopy, samples should ideally be transparent. However, most tissues or appendages appear opaque and may be coloured by pigments. These obstacles prevent imaging at high depth – or any optical penetration at all – into tissue because of light absorption and scattering, respectively (Richardson and Lichtman, 2015). Thus, sharp imaging, especially deep into a tissue volume such as from whole-mount preparations, becomes strongly limited. Alternatively, physical serial sectioning in ultra-thin slices may be performed; however, correcting single slices for alignment, geometric distortion and staining variation is time demanding and can be error prone (Zucker, 2006). Non-sectioning approaches such as optical sectioning by confocal laser scanning (cLSM) or light sheet microscopy largely preserve the innate 3D structure of biological tissues and organs, but require transparent samples (Susaki and Ueda, 2016). Although a diverse set of novel tissue-clearing techniques has been developed for some vertebrate species to achieve whole-organ or whole-body transparency, enabling imaging of fluorescence-labelled molecules deep into a large tissue volume (Chung et al., 2013; Frétaud et al., 2017; Keller and Dodt, 2012; Li et al., 2017; Susaki et al., 2014; Susaki and Ueda, 2016; Tainaka et al., 2014; Yang et al., 2014), all current clearing methods come with specific limitations, e.g. they may affect structural and molecular integrity as a result of shrinkage or swelling of cells and tissue, quenching of fluorescence and/or altered antigenicity, among other issues (Li et al., 2017; Susaki and Ueda, 2016).

In many insect species, optical imaging is especially challenging, as pigmentation prevents fluorescence-based microscopy beneath the cuticle. Pigmentation and thus coloration can vary from colourless to yellowish or brownish to black depending on the amounts and types of melanin-like pigments incorporated (Barek et al., 2017). Such pigments absorb light, which results in decreased laser intensity and low optical quality as one penetrates deeper into the tissue (Smolla et al., 2014; Zucker, 2006). This bottleneck hampers deep imaging of intact tissue, appendages or whole bodies. Physical removal of the cuticle is less desirable because of the inevitable destruction of surrounding tissue, especially in small specimens. Chemical clearing agents such as hydrogen peroxide (H_2O_2) bleach soft tissues such as brains, which allows fluorescence imaging of receptor neuron proteins by cLSM, but results in tissue shrinkage such as in ants (Smolla et al., 2014) or spherically expanded ruptures in hawkmoths (Stöckl and Heinze, 2015). Other bleaching protocols for whole insects with brownish bodies require at least 3 weeks of incubation (Kliot and Ghanim, 2016; Koga et al., 2009). As many insect species such as beetles possess a particular thick, hard and pigmented cuticle, here we present a novel methodological strategy that combines both specific and effective clearing of cuticular pigmentation as well as preservation of molecular and cellular integrity. This approach allows optical imaging of fluorescence-labelled polynucleotides in intact appendages or other whole-mount organs.

MATERIALS AND METHODS

Specimens, RNA extraction and cDNA synthesis

Poplar leaf beetles (*Chrysomela populi* Linnaeus) were collected close to Dornburg (+51°00′52″, +11°38′17″) in Thuringia, Germany, where beetles were feeding on *Populus maximowiczii*×*Populus nigra* and were reared in a climate chamber provided with fresh *P. nigra* under a 16 h:8 h light:dark cycle at 20°C. Mustard leaf beetles [*Phaedon cochleariae* (Fabricius)] were lab reared on *Brassica oleracea*. Both beetle species (Insecta: Coleoptera) belong to the tribe Chrysomelini within the family Chrysomelidae. Adult beetles were homogenised using mortar and pestle in liquid

[1]Max Planck Institute for Chemical Ecology, Department of Bioorganic Chemistry, Hans-Knöll-Str. 8, D-07745 Jena, Germany. [2]Max Planck Institute for Chemical Ecology, Department of Evolutionary Neuroethology, Hans-Knöll-Str. 8, D-07745 Jena, Germany.

*Author for correspondence (spentzold@ice.mpg.de)

S.P., 0000-0003-3101-7465; V.G., 0000-0002-0736-2771; W.B., 0000-0001-6784-2534; A.B., 0000-0001-7353-3287

Received 30 May 2018; Accepted 16 July 2018

Journal of Experimental Biology (2018) 221, jeb185710. doi:10.1242/jeb.185710

nitrogen, and RNA was purified using RNAqueous™ Total RNA Isolation Kit (Thermo Fisher Scientific Baltics UAB, Vilnius, Lithuania) including DNase treatment, following the manufacturer's instructions. RNA concentration was measured on a NanoDrop™ One (Thermo Fisher Scientific, Madison, WI, USA). Synthesis of cDNA was carried out using SuperScript™ III Reverse Transcriptase and oligo(dT)$_{20}$ (Invitrogen™, Carlsbad, CA, USA) following the manufacturer's protocol.

Identification of candidate genes and molecular cloning

Orthologues of *laccase2* (*Lac2*) or *tyrosine hydroxylase* (*TH*) in *C. populi* and *P. cochleariae* were identified by performing a BLAST search against the respective transcriptome (Stock et al., 2013; Strauss et al., 2014) using nucleotide sequences of *Lac2* (GenBank accession number: AY884061.2) and *TH* (EF592178) from *Tribolium castaneum* as the template (Arakane et al., 2005; Gorman and Arakane, 2010). As targets for RNA fluorescence *in situ* hybridisation (FISH), a gustatory receptor (*CpopGR1*) and an odorant-binding protein (*CpopOBP13*) were identified from the transcriptome of *C. populi* (Strauss et al., 2014) by a BLAST search using the template sequences CbowGR1 (GenBank: KT381521) and CbowOBP13 (KT381495) from the cabbage beetle *Colaphellus bowringi* (Li et al., 2015) (Chrysomelini, Chrysomelidae). The sequence of the housekeeping gene *actin* from *C. populi* was obtained from GenBank (JX122919.1). Gene-specific primers were designed using Primer3 software (see Table S1); a T7 promoter sequence (5′-TAATACGACTCACTATAGGGAGA-3′) was appended to forward and reverse primers of *Lac2* (*CpopLac2*, *PcoLac2*) and *TH* (*CpopTH*, *PcoTH*) to allow dsRNA synthesis for RNA interference (RNAi). PCR amplification was carried out using a proof-reading DNA polymerase (Phusion High-Fidelity F530S, Thermo Fisher Scientific). Amplicons were analysed via gel electrophoresis, purified using QIAquick PCR Purification (Qiagen, Hilden, Germany) and sequenced. After RACE-PCR to verify the full-length sequence using SMARTer RACE cDNA Amplification Kit (Clontech Laboratories, Mountain View, CA, USA), *CpopGR1*, *CpopOBP13* and *CpopActin* were PCR amplified without modification, sequenced and ligated into pCR-BluntII-TOPO (Invitrogen™) possessing opposing T7 and SP6 promoter sequences to allow *in vitro* synthesis from one template for generation of sense and antisense probes for RNA FISH (see 'Synthesis of double-labelled RNA FISH probes', below).

RNAi

Synthesis of dsRNA

Synthesis of double-stranded RNA (dsRNA) was carried out using MEGAscript® RNAi Kit (Applied Biosystems International, Zug, Switzerland) according to the manufacturer's recommendations. In brief, PCR product with opposing T7 promoters flanking the target sequences (*Lac2* and *TH* from *C. populi* or *P. cochleariae*) was transcribed *in vitro* by incubation for 6 h at 37°C with T7-Polymerase, ATP, CTP, GTP and UTP, including RNase inhibitor protein. Formation of dsRNA was induced by incubating the reaction mixture for 5 min at 75°C and then cooling to room temperature (RT). After nuclease digestion of single-stranded RNA and DNA, dsRNA was purified using filter cartridges and centrifugation. Finally, dsRNA was ethanol precipitated, resuspended in 0.9% physiological NaCl and adjusted to approximately 1 µg µl^{-1}. The concentration and integrity of the dsRNA were determined by spectrometry (NanoDrop™ One) and gel electrophoresis. The following lengths of dsRNA were generated: *Cpop*ds*TH*: 535 bp, *Cpop*ds*Lac2*: 548 bp, *Pco*ds*Lac2*: 521 bp, *Pco*ds*TH*: 544 bp (all excluding the 23 bp T7 promoter sequence; see Table S1). dsRNA of *Gfp* (719 bp) was used as a control.

Microinjection

Microinjections were performed using pulled borosilicate glass capillaries and a Nanoliter 2000 injector (both World Precision Instruments, Sarasota, FL, USA). Injection was parasagittally between the prothorax and mesothorax of either last larval instars or 3 day old pupae of *C. populi* and *P. cochleariae*. Insects were anaesthetised by chilling on ice before and during injection. Each specimen was injected with 20, 80 or 140 ng of total dsRNA. Twelve biological replicates were run per dsRNA treatment (*Lac2*, *TH*; *Gfp* as control) and amount. Additionally, 80 ng each of ds*Lac2* and ds*TH* was injected together into young pupae. Five to 10 days after eclosure and rearing of adult beetles on *P. nigra*, chemosensory appendages such as legs, antennae and palps were dissected for use in RNA FISH (see below). Additionally, the efficacy of RNAi-mediated knockdown of *CpopLac2* and *CpopTH* was assessed using quantitative real-time PCR (qPCR) on cDNA derived from the legs. Therefore, transcript abundance of *Lac2* or *TH* in ds*Gfp* control samples was set as baseline (100%) and compared with their expression in RNAi beetles (see 'qPCR', below). For statistical analysis, mean ΔΔCt (threshold cycle) values of *Lac2* or *TH* from both groups (ds*Gfp* control versus RNAi) were compared for significant differences using the Wilcoxon rank-sum test using SigmaPlot 12.0 (Systat Software, Erkrath, Germany). Five biological replicates were analysed from both groups. For primers, see Table S1.

qPCR

Using qPCR, the transcript abundance of (i) *Lac2* and *TH* was analysed in *C. populi* larvae, pupae and adults, and in adult legs, antennae and wings (three to four biological replicates), and (ii) *CpopGR1* and *CpopOBP13* in adult tissues such as gut, wings, thorax (excluding head and legs), legs, antennae and head including palps (six biological replicates). Data were quantified relative to the mRNA levels of the reference genes *eukaryotic elongation factor 1-alpha* (*EF1α*) and *initiation factor 4A* (*eIF4A*) using the $2^{-\Delta\Delta Ct}$ method (Livak and Schmittgen, 2001) and multiplied by 1000. Data were acquired on a CFX-96 Touch™ Real-Time PCR Detection System (Bio-Rad Laboratories, Hercules, CA, USA) using Brilliant III Ultra-Fast SYBR® Green QPCR Master Mix (Agilent Technologies, Cedar Creek, TX, USA) and cDNA as the template. Distilled water in place of the template served as negative control. Two technical replicates were analysed; those with a Ct difference of >0.5 were repeated. To exclude effects of RNAi (ds*Lac2*, ds*Gfp*) on the expression level of *CpopGR1* and *CpopOBP13* (as RNA FISH targets, see below), their expression was compared with that of ds*Lac2*- or ds*Gfp*-injected individuals by qPCR on cDNA derived from the legs (five biological replicates per group). The statistical difference of the ΔCt values between the two groups was compared using *t*-test (SigmaPlot 12.0, Systat Software, Erkrath, Germany). Standard curves in five different 10-fold dilutions were used to calculate the amplification efficiency. For each primer pair, sigmoidal amplification curves were obtained with single melt curve peaks. No signals were detected for the negative controls. For primers, see Table S1.

Absorbance measurement

Three legs from *C. populi* beetles that were silenced in *Lac2*, *TH* or control individuals were ground in 6 mol l^{-1} HCl and centrifuged to pellet cell and tissue debris. Supernatant was used to measure absorbance from 400 to 800 nm mg^{-1} ground

Journal of Experimental Biology (2018) 221, jeb185710. doi:10.1242/jeb.185710

tissue on a UV–Vis spectrophotometer (Jasco V-550, Jasco, Pfungstadt, Germany).

Whole-mount RNA FISH

Synthesis of double-labelled RNA FISH probes

Plasmids containing target sequences (*CpopGR1*, *CpopOBP13*, *CpopActin*) flanked by opposing T7 and SP6 promoter sequences were linearised using *Not*I or *BamH*I. Subsequent *in vitro* transcription of fluorescence-labelled antisense (test) or sense (negative control) RNA was carried out using SP6 or T7 DNA-dependent RNA polymerases (Thermo Fisher Scientific) in the presence of biotin (*GR1*, *OBP13*) or digoxigenin (DIG; *actin*) according to the RNA Labelling mix (Roche, Mannheim, Germany). After incubation for 3 h at 37°C, RNA was precipitated using ethanol, dissolved in RNase-free water and diluted in hybridisation buffer [50% deionised formamide, 2× saline sodium citrate buffer, 0.2 mg ml^{-1} UltraPure™ Herring Sperm DNA (Thermo Fisher Scientific), 200 µg ml^{-1} yeast tRNA (Roche) and 10% dextran sulfate (Calbiochem, Darmstadt, Germany) in double-distilled water]. The following probe lengths were generated: *CpopGR1*: 390 nt and *CpopOBP13*: 513 nt (both biotin labelled); and *CpopActin* (DIG labelled): about 450 nt from original 1131 nt after incubation in hydrolysis buffer (80 mmol l^{-1} $NaHCO_3$ and 120 mmol l^{-1} Na_2CO_3) at 60°C for 14.5 min (see Zimmerman et al., 2013).

Fixation and FISH procedure

Intact and whole-mount palps (labial, maxillary), antennae and legs were freshly dissected from ice-chilled adult *C. populi* beetles that were injected beforehand with ds*Lac2*, ds*TH* or ds*Gfp* as control. Three independent biological replicates from each appendage and injected dsRNA were used for FISH. To improve penetration of the labelled FISH probes, antennae and legs were cross-sectioned into a distal and proximal part (at the 5th flagellomere or between the tibia and femur, respectively). Samples were fixed in 4% paraformaldehyde in 1 mol l^{-1} $NaHCO_3$ at 4°C for 24 h. Organs were washed in 1× phosphate-buffered saline (PBS, pH 7.1) containing 0.03% Triton™ X-100 (Sigma-Aldrich, Darmstadt, Germany) for 1 min at RT and incubated in 0.2 mol l^{-1} HCl containing 0.03% Triton™ X-100 for 10 min. After washing in 1× PBS with 1% Triton™ X-100 for 1 min at RT, prehybridisation was carried out by incubating samples in hybridisation buffer for 4 h at 4°C and for an additional 6 h at 55°C. Hybridisation of labelled RNA probes to endogenous transcripts was performed at 55°C for 3 days. The following combinations were used: antisense or sense mRNA of *GR1* or *OBP13* in combination with antisense of *actin*. After washing in 0.1× saline sodium citrate buffer with 0.03% Triton™ X-100 four times at 60°C by horizontal shaking at 350 rpm, samples were blocked in 1% blocking solution (Roche) diluted in tromethamin-buffered saline (TBS, pH 7.5) and 0.03% Triton™ X-100 for 6 h at 4°C. Detection of DIG-labelled probes was achieved by using anti-DIG-conjugated alkaline phosphatase (1:500) that dephosphorylates HNPP added to the sample into HNP, which precipitates to RNA in the presence of Fast Red TR (HNPP Fluorescent Detection Set, Roche). Detection of biotin-labelled probes was achieved using streptavidin-coupled horse radish peroxidase (dilution 1:100) and tyramide signal amplification (TSA) fluorescein detection kit (Perkin Elmer, Waltham, MA, USA). In both cases, antibody incubation was carried out for 3 days at 4°C followed by substrate incubation for 6 h. Intermediate washing steps were carried out three times for 10 min in TBS with 0.05% Tween-20 (Sigma-Aldrich). Counterstaining of cellular dsDNA was done using 4′,6-diamidino-2-phenylindole (DAPI) nucleic acid stain (Molecular Probes, Eugene, OR, USA) in 30 mmol l^{-1} PBS and incubated for 30 min at RT in the dark followed by three brief washes in PBS. Finally, samples were transferred onto microscope slides covered in Vectashield® antifade mounting medium (Vector Laboratories, Burlingame, CA, USA).

Microscopy and image processing

Fluorescence images were acquired with a Zeiss LSM 880 Confocal Laser Scanning Microscope using a 20×/0.8 Plan-Apochromat or 40×/1.2 C-Apochromat W (Zeiss, Jena, Germany). Excitation of the fluorophores was conducted through a 405 nm laser diode, a 488 nm argon laser and a 543 nm helium–neon laser (Zeiss). The systems spectral Quasar detector was set up to detect the fluorophores at 415–490 nm for DAPI, 490–561 nm for biotin-labelled probes and 551–735 nm for DIG-labelled probes. The pinhole was adjusted to 1 Airy unit for the crucial channel of the *in situ* probe. Reflected light brightfield images from whole beetles or appendages were obtained on an Axio Zoom V.16 (Zeiss). Images were processed using the following imaging software: ZEN (Zeiss), Helicon Focus (HeliconSoft, Kharkiv, Ukraine), Fiji (Schindelin et al., 2012) and Photoshop® CS (Adobe Systems, San Jose, CA, USA).

Chemical bleaching

Freshly dissected and fixed antennae and legs from *C. populi* were incubated in H_2O_2 (Sigma-Aldrich) at different concentrations (aqueous 35%, 10%, 6% or alcoholic 6%) versus water or ethanol controls at RT for 3 days or 3 weeks. In addition, whole beetles were incubated in 35% H_2O_2 for 5 days at RT. For incubation in methyl salicylate, freshly dissected heads of *C. populi* were dehydrated in an ethanol series, transferred in glass vials containing 1:1 ethanol: methyl salicylate for incubation for 1 h and finally incubated in 100% methyl salicylate (Sigma-Aldrich) for 1 week at RT during shaking (350 rpm). After dehydrating further samples (legs and antennae) in a methanol series, they were incubated in a 1:2 mixture of BABB (benzyl alcohol/benzyl benzoate; Sigma-Aldrich) for 3 weeks. Two independent biological replicates were analysed for each combination.

RNA degradation

Degradation of cellular RNA was analysed from antennae and legs incubated for 3 days in 35% or 10% aqueous H_2O_2 or for 3 weeks in 6% alcoholic H_2O_2 in comparison to control incubations (water or ethanol) via qPCR after RNA extraction and cDNA synthesis from three biological replicates (5–10 antennae or legs mixed) as described above. Therefore, mean ΔΔCt values of two reference genes (*EF1α* and *eIF4A*) were compared between the two test and control treatments, taking the latter values as baseline (100%) for mRNA abundance.

RESULTS AND DISCUSSION

We took advantage of the proven functional importance of the enzymes TH and Lac2 (a phenoloxidase) in the beetle's cuticular pigmentation pathway catalysing the first and following enzymatic steps (Arakane et al., 2005; Noh et al., 2016) (Fig. 1A). As validated by qPCR, *Lac2* and *TH* were most highly expressed in the adult stage of the poplar leaf beetle (*C. populi*), especially in chemosensory appendages such as the legs and antennae, which corresponds to the highest degree of pigmentation compared with other developmental stages and tissues (Fig. S1A). Silencing *TH* and *Lac2* by RNAi resulted in significant clearing of cuticular pigmentation in

Journal of Experimental Biology (2018) 221, jeb185710. doi:10.1242/jeb.185710

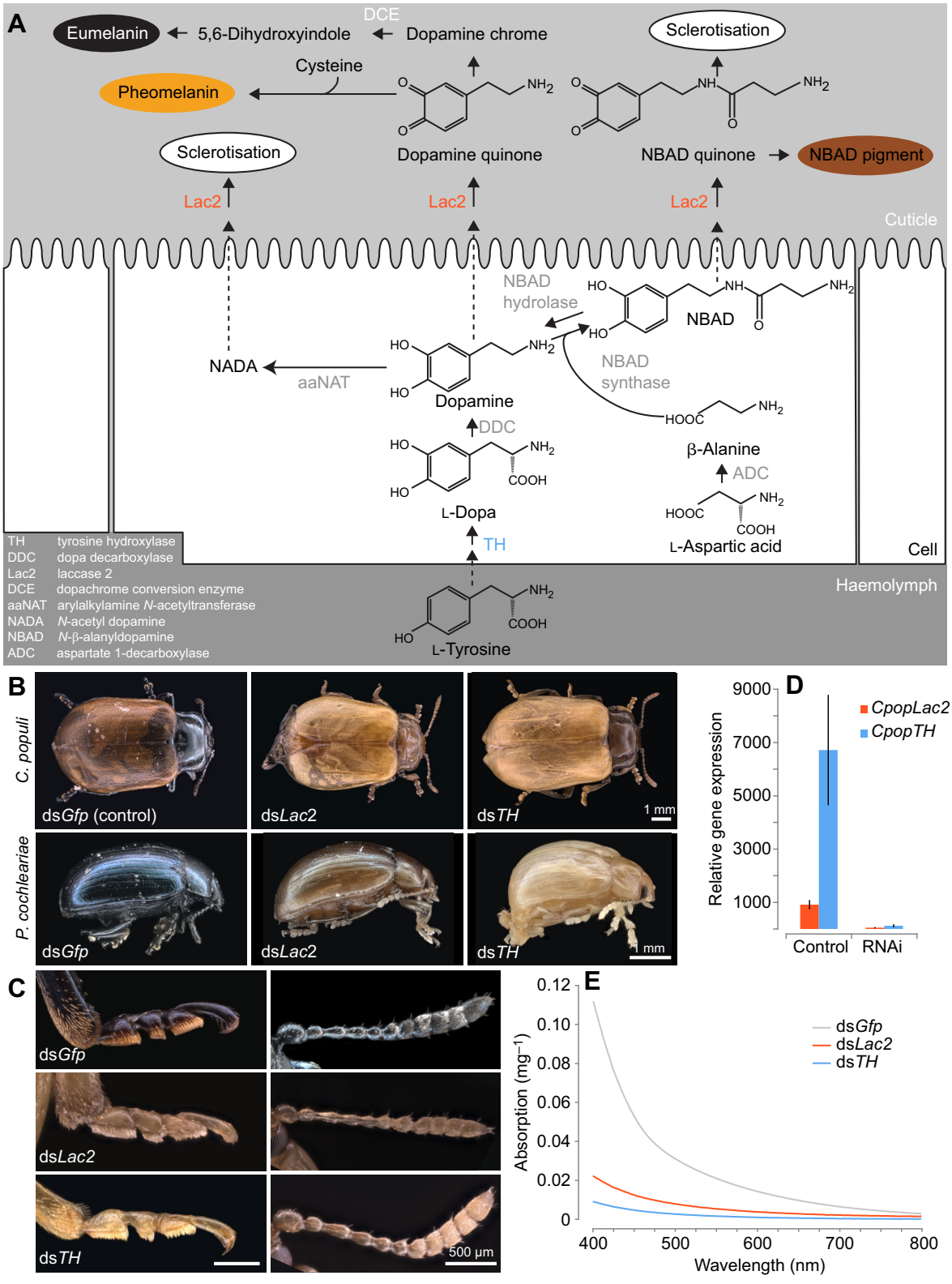

Fig. 1. See next page for legend.

comparison to RNAi controls (ds*Gfp*) in adult *C. populi* as well as the mustard leaf beetle *P. cochleariae* (Fig. 1B). Injecting 140 ng *Lac2* or *TH* dsRNA per individual was more efficient in clearing cuticular pigmentation than injecting only 80 ng dsRNA. Injection of ds*Lac2* or ds*TH* in young pupae reduced pigmentation in late pupae but not in controls (Fig. S2). Hatching rate was similar among ds*Lac2*- (68.5%, *N*=46), ds*TH*- (77.8%, *N*=22) and ds*Gfp*-injected (control, 65.8%, *N*=51) individuals. RNAi-injected adults survived at least 8 days without any apparent adverse effects. Other studies using dipteran species reported pleiotropic effects of silencing *Lac2* or *TH* such as impaired resistance (Du et al., 2017) or reduced immunity (Chen et al., 2018) after pathogenic infection.

Journal of Experimental Biology

Journal of Experimental Biology (2018) 221, jeb185710. doi:10.1242/jeb.185710

Fig. 1. Silencing expression of *tyrosine hydroxylase* (*TH*) and *laccase2* (*Lac2*) genes by RNA interference (RNAi) reduces cuticular pigmentation in adult leaf beetles. (A) The tyrosine-derived cuticular pigmentation pathway in insects, illustrating the involvement of TH (blue) and Lac2 (orange) enzymes with their respective substrates. The resulting pigments are coloured as proposed by Barek et al. (2018) and Noh et al. (2016). (B) Phenotypes of adult *Chrysomela populi* and *Phaedon cochleariae* beetles in which *Lac2* and *TH* expression was silenced by RNAi (140 ng dsRNA per individual) are less pigmented and thus paler than RNAi controls (ds*Gfp* injection). *N*=12 biological replicates per gene and species. Injection of 80 ng ds*Lac2* or ds*TH* was less efficient for clearing pigmentation, while 20 ng was not effective (not shown). (C) Detail of chemosensory appendages such as tarsi (left) and antennae (right) of RNAi-treated and control individuals, indicating cleared pigmentation. (D) Efficacy of RNAi-mediated silencing of *CpopLac2* and *CpopTH* in comparison to RNAi controls (injection of ds*Gfp*) as analysed by qPCR. Differences in relative expression are statistically significant between the two treatments (*Lac2*: *P*=0.008; *TH*: *P*=0.016; Wilcoxon rank-sum test) and refer to 94.5% and 98.2%, respectively, transcript silencing in comparison to RNAi controls. Bars represent means±s.e.m.; *N*=5 biological replicates per treatment. (E) Visible spectral changes measured by UV–Vis spectroscopy are associated with silencing of *Lac2* or *TH* by RNAi in comparison to RNAi controls (ds*Gfp*). Mean reduction in absorbance was 78% for ds*Lac2* and 91.4% for ds*TH*. Legs were macerated in acid and absorbance of the supernatant was measured from 400 to 800 nm.

Importantly, in *C. populi* and *P. cochleariae*, RNAi-based clearing of cuticular pigmentation was induced in chemosensory appendages such as antennae, legs and palps (Fig. 1B,C). Transcript levels were silenced significantly, i.e. by 94.5% and 98.2% for *CpopLac2* and *CpopTH*, respectively, in comparison to RNAi controls, as validated by qPCR (*P*=0.008, *P*=0.016; Fig. 1D).

To quantify clearing of cuticular pigmentation, the visible spectrum of the supernatant of acid-macerated legs was measured by UV–Vis spectroscopy. The higher absorbance in the 400–475 nm region in RNAi control samples, which is characteristic of brownish-coloured products from insect cuticles (Barek et al., 2017), was missing in less-pigmented *Lac2* and *TH* RNAi samples (Fig. 1E), showing a mean reduction in light absorbance of 78.0% and 91.4%, respectively. Therefore, we tested whether RNAi-cleared specimens are suitable for whole-mount RNA FISH and optical imaging by cLSM without chemical bleaching that would probably degrade mRNA.

Two distinct chemosensory gene families were chosen as RNA FISH targets: a gustatory receptor (*CpopGR1*) and an odorant-binding protein (*CpopOBP13*). Both genes were most expressed in body appendages such as the head (including palps), legs and antennae (Fig. S1B). Similar to other gene expression studies in beetles (Dippel et al., 2016; Dippel et al., 2014; Li et al., 2015), *CpopGR1* had relative low overall expression levels, even in chemosensory organs (~10% of reference genes), whereas odorant-binding proteins such as *CpopOBP13* are generally expressed more highly, as shown for the chemosensory appendages of *C. populi* (up to 15 times higher expression than that of reference genes). RNAi treatment did not affect RNA FISH target sequences, i.e. the expression levels of *GR1* and *OBP13* did not differ between RNAi-treated individuals (ds*Lac2*) compared with RNAi controls (*P*=0.39 for *CpopGR1*; *P*=0.73 for *CpopOBP13*, *t*-test). For double-labelled RNA FISH, whole-mount chemosensory appendages (palps, antennae and legs) from *Lac2* RNAi and *TH* RNAi-cleared beetles were incubated with biotin-labelled antisense mRNA (or sense mRNA as control) targeting either *CpopGR1* or *CpopOBP13* and combined with DIG-labelled *CpopActin* as housekeeping gene. Importantly, gene expression of *CpopActin*, *CpopGR1* and *CpopOBP13* in intact appendages was successfully imaged via cLSM in those individuals in which *Lac2* or *TH* expression was silenced (Fig. 2A; Fig. S3A,B). For example, cells expressing *CpopGR1* were mainly proximal in the palp (Fig. 2Ai) and overall less abundant than those expressing *CpopOBP13*, which showed a broader distribution (Fig. 2Aii). This is similar to the expression measured via qPCR, indicating relatively low and high expression for *CpopGR1* and *CpopOBP13*, respectively (Fig. S1B). Furthermore, in the antennae, *CpopOBP13* was expressed in the proximal and more distal parts (Fig. S3A), whereas in the tibia, *CpopOBP13* was mainly expressed in proximal cells (Fig. S3B). Cuticular autofluorescence in RNAi-cleared organs remained to some extant after optical sectioning by cLSM (e.g. Fig. 2Ai, Aii), which is most likely caused by chitin (Rabasović et al., 2015). In another study, H_2O_2-based quenching of autofluorescence was used to image microbial endosymbionts living in inner insect tissues such as the gut (Koga et al., 2009); in general, many tissue-clearing methods do not necessarily remove background autofluorescence (Richardson and Lichtman, 2015). In contrast to RNAi-cleared specimens, optical imaging of *CpopActin*, *CpopGR1* and *CpopOBP13* was not possible in RNAi controls (ds*Gfp*) because of retained pigmentation that prevented optical penetration (Fig. 2Aiii). As further controls, using sense mRNA for FISH did not result in specific fluorescence for *GR1* or *OBP13* in any of the RNAi-treated beetles (ds*Lac2*, ds*TH* or ds*Gfp* controls) (Fig. 2A; Fig. S3C). Nuclear DNA staining via fluorescent DAPI confirmed cell integrity in RNAi-cleared tarsi of *C. populi* and *P. cochleariae* (Fig. 2B).

To corroborate that RNAi-based clearing of cuticular pigmentation is the method choice with whole-mount organs in RNA FISH, we showed that several bleaching chemicals are not feasible for FISH, because of significant degradation of polynucleotides, lack of clearing efficacy or long incubation times. We first tested H_2O_2, of which hydroxyl radicals and OOH groups are known to destroy the cuticle pigment melanin (Korytowski and Sarna, 1990). Whereas incubation of dissected body appendages in 35% H_2O_2 for 3 days reduced cuticular pigmentation in the legs (Fig. 2C), it degraded 99.2% of the total RNA in comparison to water-incubated controls (Fig. 2D); similarly, antennae were chemically bleached, resulting in degradation of 91.6% of total RNA (Fig. 2C,D). Incubation of antennae and legs for 3 days in water (Fig. 2C) or 10% H_2O_2 did not reduce cuticular pigmentation but did degrade RNA (Fig. 2D). Incubation in alcoholic 6% H_2O_2 took at least 3 weeks to cause bleaching of intact or bipartite antennae and legs (Fig. S4A). This is a similar length to bleaching brown-coloured but relatively small insects such as lice, bat flies or aphids (Koga et al., 2009). However, almost two-thirds of total RNA (63.7%) was degraded despite prior tissue fixation. When whole beetles were incubated in 35% H_2O_2 for 5 days, cuticular decoloration was evident, but partly incomplete, especially on the legs and wings, which were also damaged (Fig. S4B). Consequently, cell integrity in the legs and antennae was not retained in H_2O_2-bleached samples as further indicated by unsuccessful DAPI staining (Fig. 2E). The cell-damaging characteristics of H_2O_2 resulting in degradation of total RNA and decreased fluorescence emission from green fluorescent proteins (Alnuami et al., 2008), makes this bleaching method unsuitable for (RNA) FISH. This is especially important when targeting genes expressed at a low level, such as most insect GRs (Dippel et al., 2016). Other clearing agents such as methyl salicylate (Zucker, 2006) did clear soft tissues such as the brain of *C. populi*, but retained cuticular pigmentation (Fig. S5A). Similarly, a mixture of benzyl alcohol/benzyl benzoate did not clear cuticular pigmentation in antennae or legs (Fig. S5B).

Overall, RNAi-based clearing of cuticular pigmentation is a significant improvement compared with chemical bleaching agents,

Journal of Experimental Biology (2018) 221, jeb185710. doi:10.1242/jeb.185710

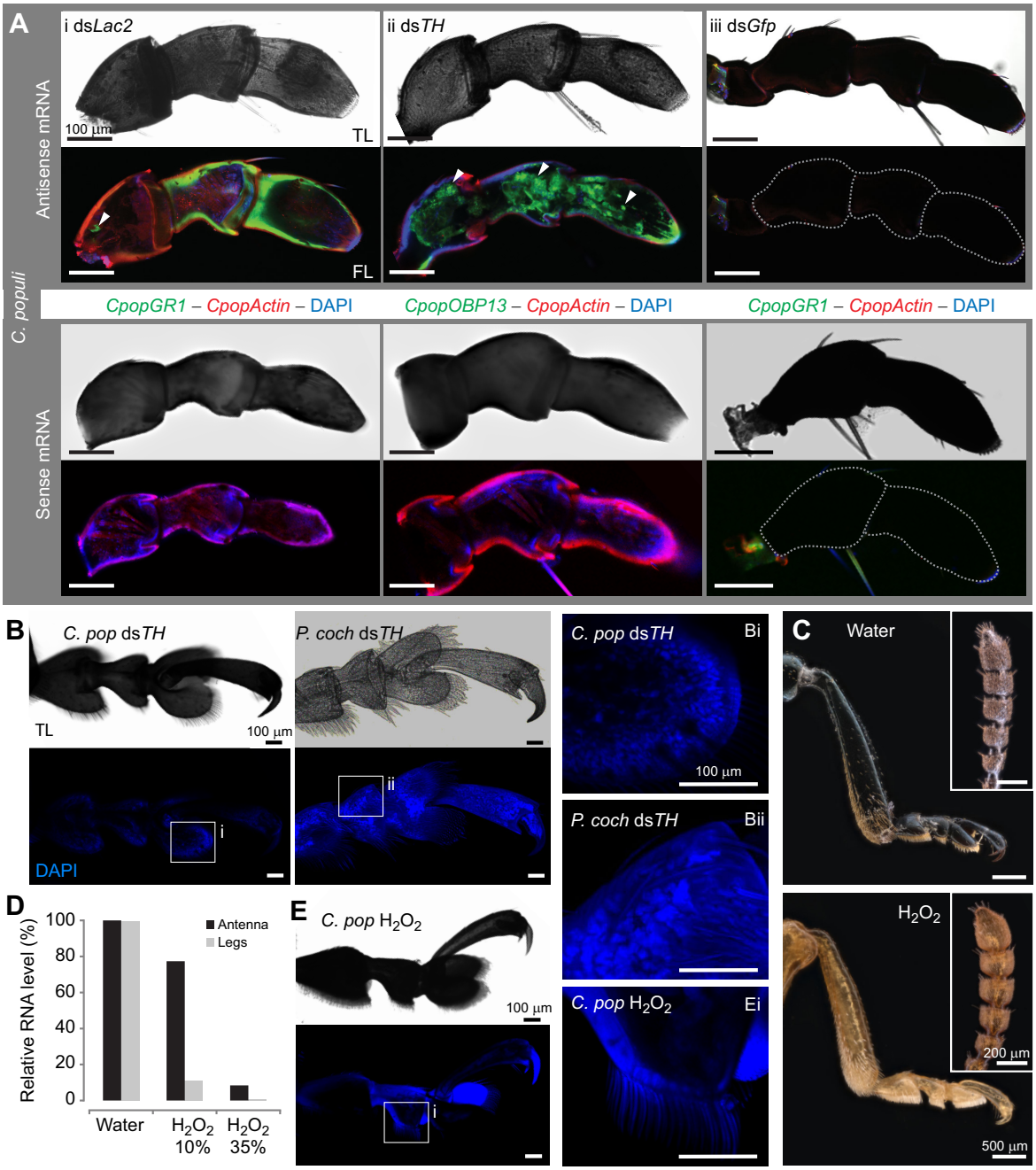

Fig. 2. Specific clearing of cuticular pigmentation by RNAi enables RNA fluorescence *in situ* hybridisation (FISH) in whole-mount appendages of leaf beetles. (A) Maxillary palps from (i) *Lac2*- or (ii) *TH*-silenced individuals with biotin-labelled mRNA of either a gustatory receptor (*CpopGR1*) or an odorant-binding protein (*CpopOBP13*) (both green) in combination with digoxigenin-labelled mRNA for *CpopActin* (red) as well as nuclear staining via DAPI (blue fluorescence). Because of pigmentation remaining in RNAi controls (ds*Gfp*, iii) optical imaging by FISH using the same mRNA probes was not possible. Whereas antisense mRNA binds to the target sequence (upper panels, arrowheads), sense mRNA of *GR1* or *OBP13* as control does not bind (lower panels). TL, transmitted light microscopy (light panels); FL, fluorescence image from confocal laser scanning microscopy (dark panels). (B) Tarsi of *C. populi* (left, i) and *P. cochleariae* (right, ii) cleared by silencing *TH* and stained with DAPI (targeting nuclear dsDNA) confirms cellular integrity following RNAi treatment. (C) Incubation of antennae and legs of *C. populi* in H_2O_2 (35%) for 3 days clears cuticular pigmentation in comparison to water controls, but (D) results in degradation of total RNA in both organs (bars represent mean of three biological replicates per treatment). (E) Tarsi incubated in H_2O_2 for 3 days could not be stained by DAPI, indicating cellular damage by H_2O_2. Fluorescence is cuticular autofluorescence (i). *N*=3 biological replicates for each treatment.

as it preserves molecular and cellular integrity and enables optical imaging of FISH probes deep into tissue of intact whole-mount samples. This makes serial sectioning of organs redundant. We expect that our method (termed RNA-i-FISH) would also work with other, non-chemosensory genes as FISH targets regardless of whether they encode soluble proteins or membrane receptors, or whether they are expressed at a low or high level. Moreover, as RNAi-based suppression of *Lac2* or *TH* decreases cuticular pigmentation in different coleopteran (Gorman and Arakane, 2010; Niu et al., 2008; Powell et al., 2017) and several non-coleopteran insect species (Chen et al., 2018; Elias-Neto et al., 2010; Futahashi et al., 2011; Liu et al., 2010; Okude et al., 2017),

our method could be adapted to many other hexapod species, enabling investigations beyond transparent embryos or ovaries. Imaging beneath the RNAi-cleared cuticle may further benefit from light sheet microscopy, which minimizes fluorophore bleaching and phototoxic effects. Finally, RNAi-based cuticle clearing complements existing toolkits by, for example, enabling *in vivo* calcium imaging, in contrast to chemical bleaching, which does not maintain most life functions.

Acknowledgements
We are grateful to Vera L. Hopfenmüller for running replicates of FISH and to Tobias Becker for setting up the absorbance measurement.

Competing interests
The authors declare no competing or financial interests.

Author contributions
Conceptualization: S.P., W.B., A.B.; Methodology: S.P., V.G., A.O., L.S., A.B.; Validation: S.P., V.G., A.O., L.S.; Formal analysis: S.P., V.G., A.O.; Investigation: S.P., V.G., A.O., L.S.; Data curation: S.P.; Writing - original draft: S.P.; Writing - review & editing: S.P., V.G., W.B., A.B.; Visualization: S.P., V.G.; Supervision: S.P., W.B., A.B.; Project administration: S.P., A.B.; Funding acquisition: S.P., W.B., A.B.

Funding
S.P. and A.B. received project funding from the European Union's Horizon 2020 research and innovation programme under the Marie Skłodowska-Curie grant agreement no. 705151. Further financial support to all authors from the Max Planck Society is acknowledged.

Data availability
The data that support the findings of this study are available from the corresponding author upon reasonable request. Sequences generated in this study have been deposited in GenBank (www.ncbi.nlm.nih.gov/genbank) under the following accession numbers: *CpopLac2*: MH253687; *PcoLac2*: MH253688; *CpopTH*: MH253689; *PcoTH*: MH253690; *CpopGR1*: MH253691; and *CpopOBP13*: MH253692.

Supplementary information
Supplementary information available online at
http://jeb.biologists.org/lookup/doi/10.1242/jeb.185710.supplemental

References
Alnuami, A. A., Zeedi, B., Qadri, S. M. and Ashraf, S. S. (2008). Oxyradical-induced GFP damage and loss of fluorescence. *Int. J. Biol. Macromol.* **43**, 182-186.

Arakane, Y., Muthukrishnan, S., Beeman, R. W., Kanost, M. R. and Kramer, K. J. (2005). Laccase 2 is the phenoloxidase gene required for beetle cuticle tanning. *Proc. Natl. Acad. Sci. USA* **102**, 11337-11342.

Barek, H., Evans, J. and Sugumaran, M. (2017). Unraveling complex molecular transformations of N-β-alanyldopamine that accounts for brown coloration of insect cuticle. *Rapid Commun. Mass Spectrom.* **31**, 1363-1373.

Barek, H., Sugumaran, M., Ito, S. and Wakamatsu, K. (2018). Insect cuticular melanins are distinctly different from those of mammalian epidermal melanins. *Pigment Cell Melanoma Res.* **31**, 384-392.

Chen, E.-H., Hou, Q.-L., Wei, D.-D., Dou, W., Liu, Z., Yang, P.-J., Smagghe, G. and Wang, J.-J. (2018). Tyrosine hydroxylase coordinates larval-pupal tanning and immunity in oriental fruit fly (*Bactrocera dorsalis*). *Pest Manage. Sci.* **74**, 569-578.

Chung, K., Wallace, J., Kim, S.-Y., Kalyanasundaram, S., Andalman, A. S., Davidson, T. J., Mirzabekov, J. J., Zalocusky, K. A., Mattis, J., Denisin, A. K. et al. (2013). Structural and molecular interrogation of intact biological systems. *Nature* **497**, 332-337.

Dippel, S., Oberhofer, G., Kahnt, J., Gerischer, L., Opitz, L., Schachtner, J., Stanke, M., Schütz, S., Wimmer, E. A. Angeli, S. (2014). Tissue-specific transcriptomics, chromosomal localization, and phylogeny of chemosensory and odorant binding proteins from the red flour beetle *Tribolium castaneum* reveal subgroup specificities for olfaction or more general functions. *BMC Genomics* **15**, 1141.

Dippel, S., Kollmann, M., Oberhofer, G., Montino, A., Knoll, C., Krala, M., Rexer, K.-H., Frank, S., Kumpf, R., Schachtner, J. et al. (2016). Morphological and transcriptomic analysis of a beetle chemosensory system reveals a gnathal olfactory center. *BMC Biol.* **14**, 90.

Du, M.-H., Yan, Z.-W., Hao, Y.-J., Yan, Z.-T., Si, F.-L., Chen, B. and Qiao, L. (2017). Suppression of Laccase 2 severely impairs cuticle tanning and pathogen resistance during the pupal metamorphosis of *Anopheles sinensis* (Diptera: Culicidae). *Parasit. Vectors* **10**, 171.

Elias-Neto, M., Soares, M. P. M., Simões, Z. L. P., Hartfelder, K. and Bitondi, M. M. G. (2010). Developmental characterization, function and regulation of a Laccase2 encoding gene in the honey bee, *Apis mellifera* (Hymenoptera, Apinae). *Insect Biochem. Mol. Biol.* **40**, 241-251.

Frétaud, M., Rivière, L., De Job, É., Gay, S., Lareyre, J.-J., Joly, J.-S., Affaticati, P. and Thermes, V. (2017). High-resolution 3D imaging of whole organ after clearing: taking a new look at the zebrafish testis. *Sci. Rep.* **7**, 43012.

Futahashi, R., Tanaka, K., Matsuura, Y., Tanahashi, M., Kikuchi, Y. and Fukatsu, T. (2011). Laccase2 is required for cuticular pigmentation in stinkbugs. *Insect Biochem. Mol. Biol.* **41**, 191-196.

Gorman, M. J. and Arakane, Y. (2010). Tyrosine hydroxylase is required for cuticle sclerotization and pigmentation in *Tribolium castaneum*. *Insect Biochem. Mol. Biol.* **40**, 267-273.

Keller, P. J. and Dodt, H.-U. (2012). Light sheet microscopy of living or cleared specimens. *Curr. Opin. Neurobiol.* **22**, 138-143.

Kliot, A. and Ghanim, M. (2016). Fluorescent in situ hybridization for the localization of viruses, bacteria and other microorganisms in insect and plant tissues. *Methods* **98**, 74-81.

Koga, R., Tsuchida, T. and Fukatsu, T. (2009). Quenching autofluorescence of insect tissues for in situ detection of endosymbionts. *Appl. Entomol. Zool.* **44**, 281-291.

Korytowski, W. and Sarna, T. (1990). Bleaching of melanin pigments. Role of copper ions and hydrogen peroxide in autooxidation and photooxidation of synthetic dopa-melanin. *J. Biol. Chem.* **265**, 12410-12416.

Lampasona, A. A. and Czaplinski, K. (2016). RNA voyeurism: a coming of age story. *Methods* **98**, 10-17.

Li, X.-M., Zhu, X.-Y., Wang, Z.-Q., Wang, Y., He, P., Chen, G., Sun, L., Deng, D.-G. and Zhang, Y.-N. (2015). Candidate chemosensory genes identified in *Colaphellus bowringi* by antennal transcriptome analysis. *BMC Genomics* **16**, 1028.

Li, W., Germain, R. N. and Gerner, M. Y. (2017). Multiplex, quantitative cellular analysis in large tissue volumes with clearing-enhanced 3D microscopy (Ce3D). *Proc. Natl. Acad. Sci. USA* **114**, E7321-E7330.

Liu, C., Yamamoto, K., Cheng, T.-C., Kadono-Okuda, K., Narukawa, J., Liu, S.-P., Han, Y., Futahashi, R., Kidokoro, K., Noda, H. et al. (2010). Repression of tyrosine hydroxylase is responsible for the sex-linked chocolate mutation of the silkworm, *Bombyx mori*. *Proc. Natl. Acad. Sci. USA* **107**, 12980-12985.

Livak, K. J. and Schmittgen, T. D. (2001). Analysis of relative gene expression data using real-time quantitative PCR and the $2^{-(\Delta\Delta CT)}$ method. *Methods* **25**, 402-408.

Niu, B.-L., Shen, W.-F., Liu, Y., Weng, H.-B., He, L.-H., Mu, J.-J., Wu, Z.-L., Jiang, P., Tao, Y.-Z. and Meng, Z.-Q. (2008). Cloning and RNAi-mediated functional characterization of MaLac2 of the pine sawyer, *Monochamus alternatus*. *Insect Mol. Biol.* **17**, 303-312.

Noh, M. Y., Muthukrishnan, S., Kramer, K. J. and Arakane, Y. (2016). Cuticle formation and pigmentation in beetles. *Curr. Opin. Insect Sci.* **17**, 1-9.

Okude, G., Futahashi, R., Kawahara-Miki, R., Yoshitake, K., Yajima, S. and Fukatsu, T. (2017). Electroporation-mediated RNA interference reveals a role of the multicopper oxidase 2 gene in dragonfly cuticular pigmentation. *Appl. Entomol. Zool.* **52**, 379-387.

Powell, M. E., Bradish, H. M., Gatehouse, J. A. and Fitches, E. C. (2017). Systemic RNAi in the small hive beetle *Aethina tumida* Murray (Coleoptera: Nitidulidae), a serious pest of the European honey bee *Apis mellifera*. *Pest Manage. Sci.* **73**, 53-63.

Rabasović, M. D., Pantelić, D. V., Jelenković, B. M., Ćurčić, S. B., Rabasović, M. S., Vrbica, M. D., Lazović, V. M., Ćurčić, B. P. M. and Krmpot, A. J. (2015). Nonlinear microscopy of chitin and chitinous structures: a case study of two cave-dwelling insects. *J. Biomed. Opt.* **20**, 016010.

Richardson, D. S. and Lichtman, J. W. (2015). Clarifying tissue clearing. *Cell* **162**, 246-257.

Schindelin, J., Arganda-Carreras, I., Frise, E., Kaynig, V., Longair, M., Pietzsch, T., Preibisch, S., Rueden, C., Saalfeld, S., Schmid, B. et al. (2012). Fiji: an open-source platform for biological-image analysis. *Nat. Methods* **9**, 676.

Smolla, M., Ruchty, M., Nagel, M. and Kleineidam, C. J. (2014). Clearing pigmented insect cuticle to investigate small insects' organs in situ using confocal laser-scanning microscopy (cLSM). *Arthropod Struct. Dev.* **43**, 175-181.

Stock, M., Gretscher, R. R., Groth, M., Eiserloh, S., Boland, W. and Burse, A. (2013). Putative sugar transporters of the mustard leaf beetle *Phaedon cochleariae*: their phylogeny and role for nutrient supply in larval defensive glands. *PLoS ONE* **8**, e84461.

Stöckl, A. L. and Heinze, S. (2015). A clearer view of the insect brain—combining bleaching with standard whole-mount immunocytochemistry allows confocal imaging of pigment-covered brain areas for 3D reconstruction. *Front. Neuroanat.* **9**, 121.

Strauss, A. S., Wang, D., Stock, M., Gretscher, R. R., Groth, M., Boland, W. and Burse, A. (2014). Tissue-specific transcript profiling for ABC transporters in the sequestering larvae of the phytophagous leaf beetle *Chrysomela populi*. *PLoS ONE* **9**, e98637.

Susaki, E. A. and Ueda, H. R. (2016). Whole-body and whole-organ clearing and imaging techniques with single-cell resolution: toward organism-level systems biology in mammals. *Cell Chem. Biol.* **23**, 137-157.

Susaki, E. A., Tainaka, K., Perrin, D., Kishino, F., Tawara, T., Watanabe, T. M., Yokoyama, C., Onoe, H., Eguchi, M., Yamaguchi, S. et al. (2014). Whole-brain imaging with single-cell resolution using chemical cocktails and computational analysis. *Cell* **157**, 726-739.

Tainaka, K., Kubota, S. I., Suyama, T. Q., Susaki, E. A., Perrin, D., Ukai-Tadenuma, M., Ukai, H. and Ueda, H. R. (2014). Whole-body imaging with single-cell resolution by tissue decolorization. *Cell* **159**, 911-924.

Yang, B., Treweek, J. B., Kulkarni, R. P., Deverman, B. E., Chen, C.-K., Lubeck, E., Shah, S., Cai, L. and Gradinaru, V. (2014). Single-cell phenotyping within transparent intact tissue through whole-body clearing. *Cell* **158**, 945-958.

Zimmerman, S. G., Peters, N. C., Altaras, A. E. and Berg, C. A. (2013). Optimized RNA ISH, RNA FISH and protein-RNA double labeling (IF/FISH) in drosophila ovaries. *Nat. Protoc.* **8**, 2158.

Zucker, R. M. (2006). Whole insect and mammalian embryo imaging with confocal microscopy: morphology and apoptosis. *Cytometry A* **69A**, 1143-1152.